STEP	ERROR REDUCTION RECOMMENDATIONS		
	PROCEDURES	TRAINING	EQUIPMENT
2.1 Verify tanker is empty	Double check via unladen weight check. Use checklist	Stress importance of verifying tanker is empty	Provide gauge indicating tanker pressure
2.3 Enter tanker target weight	Independent validation of target weight. Recording of values in checklist	Ensure operator double checks entered date	Automatic setting of weight alarms from unladen weight. Computerise logging system and build in checks on tanker reg. no. and unladen weight linked to warning system. Display differences between unladen and current weights
3.2.2 Check Road Tanker while filling	Provide secondary task involving other personnel. Supervisor periodically checks operation	Stress importance of regular checks for safety	Provide automatic log-in procedure
3.2.3 Attend tanker during filling of last 2-3 tonnes (on weight alarm)	Ensure work schedule allows operator to do this without pressure	Illustrate consequences of not attending	Repeat alarm in secondary area. Automatic interlock to terminate loading if alarm not acknowledged. Visual indication of alarm.
3.2.5 Cancel final weight alarm	Note differences between the sound of the two alarms in checklist	Alert operators during training about differences in sounds of alarms	Use completely different tones for initial and final weight alarms

Figure 9: Error Reduction Recommendations

ADVANCES IN GAS CLOUD DISPERSION MODELLING: HEAVY CLOUDS ON SLOPING GROUND

D.M.Webber, S.J.Jones, and D.Martin
SRD, AEA Technology, Wigshaw Lane, Culcheth, Warrington WA3 4NE

A model is presented of the motion of a heavy gas cloud down a uniform slope in calm ambient conditions. The model is derived from solutions of the shallow water equations with appropriate boundary conditions. Its predictions are shown to agree adequately with experimental results in calm conditions, and a possible generalisation to allow for the presence of a wind is discussed.

Keywords: Gas Cloud, Sloping Ground.

1 INTRODUCTION

Integral (or box) models of gas dispersion are now a standard tool for the analysis of flammable and toxic hazards, posed by major industrial plant. Recent developments, including work under the recently completed Major Technological Hazards programme of the Commission of the European Communities, have been aimed at extending the understanding of heavy gas flows to situations where the nature of the terrain, or of structures on it, may have a significant effect on the dispersion. The results of the CEC project have been sumarised by Builtjes (1992) who gives full reference to the more complete reports of the individual participants. This work includes: field trials on propane clouds, with and without momentum at the source, encountering fence and channel obstacles; wind–tunnel experiments involving many repeated releases, clouds encountering fences, and clouds on sloping ground; analysis of earlier data on the interction of clouds with obstacles, and analysis of concentration fluctuations in earlier experiments; and mathematical modelling of some of these processes.

Here we shall focus on some aspects of gas clouds released on sloping ground. The work presented was begun under the above project. Hazardous clouds are very often significantly heavier than air and such sloping terrain is known to have a important effect. Models of the behaviour of a heavy cloud released instantaneously on a slope have recently been presented by Deaves and Hall (1990) and by Nikmo and Kukkonen (1991).

Each of these models is an intuitively appealing generalisation of the flat ground integral model approach to include the effects of slopes. However, in each case the effect of the slope is only found with a numerically computed solution to a set of differential equations. Whilst this situation is quite usual, it is highly desirable to have a more direct understanding of the nature and effects of the assumptions involved in such models.

The importance of such an understanding cannot be overstated. Credible hazard analysis can only come about using models which are well validated on (of necessity) small scale data, and which incorporate sound physical assumptions (and accurate calculational methods) in

extrapolating their predictions to larger scales. In situations where data are relatively sparse, and the possible validation therefore relatively incomplete, the importance of the sound physical assumptions is highlighted still further.

Our objective here, then, is to examine the very simple case of a heavy cloud released instantaneously on to a uniform slope and dispersing isothermally in a way which is known to conserve buoyancy. We shall focus here on the effect of the slope on the overall motion of the cloud, rather than on any effect it may have on dilution rates. In order to do this, we shall start by discarding all other complicating factors. We therefore restrict ourselves *a priori* to the case of zero wind, and idealise to the extent that no mixing is assumed. This, as we shall show, allows considerable progress in understanding the effect of the cloud falling down the slope.

In particular an equation is derived relating the cloud's terminal velocity down the slope (where gravity balances resistance forces) to its density and volume, and to the gradient of the slope. Comparison with data will show that this assumption yields very plausible results.

2 TWO-DIMENSIONAL RELEASES ON SLOPES

2.1 Introduction

Our main purpose is to present results for the case of a three-dimensional cloud released instantaneously. It is instructive, however, first to consider the simpler two-dimensional case, discussed by Jones, Martin, Webber, and Wren (1991).

The essential assumption of our approach is that it is reasonable to consider the motion of a cloud on a slope, independently of its mixing with the ambient air. Thus we are attempting to assess how a (fictitious) cloud of fixed density might behave on a slope. Of course, any complete model of gas cloud behaviour must model mixing accurately, and we shall return to a discussion of this below.

The behaviour of a cloud of fixed density is readily accessible via the shallow water equations, which contain the added assumptions that the cloud is of large horizontal extent compared with its depth, and that the slope is not too steep. That is to say, if we designate the fluid depth as H, the horizontal extent Λ, and the gradient of the slope Γ: we require $H \ll \Lambda$ and $\Gamma \ll 1$. Later we shall discuss the regimes $H=O(\Gamma\Lambda)$ and $H \gg O(\Gamma\Lambda)$. Let us note here that these are not incompatible with the formal restrictions imposed by shallow water theory. For our purposes here, when we refer to a "tall" cloud we mean $H \gg O(\Gamma\Lambda)$ rather than one which violates the shallow ($H \ll \Lambda$) assumption.

2.2 The Two-Dimensional Shallow-Water Model

The shallow water equations in one horizontal dimension (implying a two-dimensional flow when the vertical, depth-averaged dimension is counted) are:

$$\frac{\partial(h-a)}{\partial t} + \frac{\partial(u(h-a))}{\partial x} = 0 \qquad (2.1)$$

$$\frac{\partial u}{\partial t} + u\frac{\partial u}{\partial x} + g''\frac{\partial h}{\partial x} = 0 \qquad (2.2)$$

Here t is time, and x is the horizontal space coordinate. The fields are the horizontal velocity u and the height h of the top of the cloud above a fixed datum (see Figure 1). The quantity a, is the height of the ground level above the datum, so that h-a is the fluid depth. We are considering a cloud of density ρ spreading in an ambient atmosphere of density ρ_a and g" is the reduced acceleration due to gravity

$$g'' = g\frac{\rho - \rho_a}{\rho} \qquad (2.3)$$

In the case studied here, as mixing is not yet incorporated into the model, g" is constant.

The fact that there will be significant resistance exerted by the ambient air to the cloud spread is embodied in the boundary conditions. This resistance to motion can be incorporated (Wheatley and Webber 1984, Fannelop and Jacobsen 1984, Grundy and Rottman 1985, Webber and Brighton 1986) in the boundary condition

$$u_f = k_f\sqrt{g'(h-a)_f} \qquad (2.4)$$

where g' is defined, (slightly differently from g") by

$$g' = g\frac{\rho - \rho_a}{\rho_a} \qquad (2.5)$$

and $(h-a)_f$, u_f are the fluid depth and (normal component of) velocity at the edge of the cloud, and k_f is a constant (O(1)) Froude number. (Note that k_f is not identical to the similar quantity used in integral models, which is based on the mean depth rather than the frontal depth; for self similar flow the two Froude constants have a constant ratio.) This boundary condition expresses a resistance pressure of the ambient air and we shall adopt it wherever the cloud edge is moving into the ambient fluid.

Where the cloud edge is receding from the ambient fluid we shall adopt the boundary condition

$$h_f = 0 \tag{2.6}$$

allowing movement of the trailing edge without resistance.

Here we shall consider only a uniform slope, downwards in the direction of increasing x, given by

$$a(x) = -\Gamma x \tag{2.7}$$

where the slope Γ is constant and positive.

2.3 Analytic Solution of the Shallow Water Equations

As we have seen (Jones, Martin, Webber, and Wren 1991), there is a very simple analytic solution of the above problem, representing a wedge of gas moving downhill at its terminal velocity (corresponding to a balance of gravity and resistance forces). The derivation of this is briefly as follows.

Assume there is a "terminal velocity" solution in which the fluid velocity is independent of both time and space. If this is the case, then the first of the two shallow water equations becomes

$$\left(\frac{\partial}{\partial t} + u\frac{\partial}{\partial x}\right)(h-a) = 0 \tag{2.8}$$

and the solution must have the form

$$(h - a) = H(x - ut) \tag{2.9}$$

for some function H. At the rear boundary, $x=X_b(t)$, which follows the cloud, the fluid height is zero, so that

$$H(X_b - ut) = 0 \tag{2.10}$$

and the origin of the coordinate system can now be chosen so that $X_b = ut$. The boundary condition at the front is

$$(h - a)_f = \frac{u_f^2}{g'k_f^2} \tag{2.11}$$

and this can now be rewritten as

$$H(X_f - ut) = \frac{u_f^2}{g'k_f^2} \tag{2.12}$$

where X_f is the position of the front of the fluid region. The right hand side of this equation is constant, as the velocity is constant (by assumption), and therefore the left hand side of this equation has to be constant. If the extent of the gas cloud is $L = X_f - X_b$ then:

$$H(L) = \frac{u^2}{g'k_f^2} \tag{2.13}$$

and L must therefore be constant. Note also from (2.11) that a solution with constant u implies constant frontal depth.

The second equation of the two shallow water equations can be written as

$$\frac{\partial u}{\partial t} + u\frac{\partial u}{\partial x} = -g''\left(\frac{\partial(h-a)}{\partial x} - \Gamma\right) \tag{2.14}$$

With the velocity u assumed independent of space and time, this equation reduces to

$$\frac{\partial(h-a)}{\partial x} = \Gamma \tag{2.15}$$

where $\Gamma = -da/dx$ is the gradient of the slope as defined above. With h−a of the above form H(x−ut), then clearly we must have

$$H(x - ut) = \Gamma.[x - ut] \tag{2.16}$$

up to a possible additive constant, (which is simply equivalent to a choice of origin). The front depth $(h-a)_f$ is now just ΓL, and so the front condition gives the terminal velocity

$$u = k_f[\Gamma g' L]^{1/2} \tag{2.17}$$

It is convenient to define the two−dimensional volume V of the cloud (the volume per unit width or side area). For the above solution this is just

$$V = \frac{L^2\Gamma}{2} \tag{2.18}$$

In terms of this, the cloud moves at a speed

$$u = 2^{1/4} k_f \Gamma^{1/4} [g'^2 V]^{1/4} \tag{2.19}$$

The last factor can be anticipated from dimensional analysis, but this result does show that the heavy gas cloud (of a given volume and density) moves down the slope with a terminal velocity proportional to the fourth root of the gradient of the slope.

2.4 Numerical Solution of the Shallow Water Equations

It is worth emphasising that the above analytic solution was originally found after a numerical solution had revealed this very simple asymptotic behaviour at large time. This demonstrates that the solution is indeed a stable one, and is therefore valid within the assumptions.

The evolution found for a wedge released from rest is shown in Figures 2a–2d. These figures illustrate the initial acceleration of the head; the subsequent formation of a hydraulic jump separating distinct head and tail regions; the evolution of the tail region as it then catches up with the head; and finally the collapse of the hydraulic jump leaving a wedge of material moving down the hill *en masse* with a level top surface and constant uniform velocity.

2.5 Comment

The solution of the shallow water equations discussed above is peculiar in that the cloud doesn't spread. This is a consequence of the boundary conditions, combined with the existence of a slope. The motion of the down slope edge, is just as one would expect for a cloud on flat ground; the collapse of the upslope edge, and the subsequent H=0 boundary condition, does not constrain its velocity, allowing it simply to follow the fluid motion. In this way the slumping is turned into a bulk downhill motion. It is thus clear how the assumptions built into the model can yield this result, which we feel is eminently plausible.

3 THREE–DIMENSIONAL RELEASES ON SLOPES

3.1 The Shallow Water model

The two–dimensional model of Section 2 is interesting but very restrictive. More interesting is the corresponding evolution of a three–dimensional cloud released on the slope. Our numerical

scheme for solving shallow water equations cannot yet cope with three dimensions (two horizontal dimensions) but, as we shall now show, there does exist an almost equally simple analytic solution in this case.

Consider first the cross–slope dimension. At first one might imagine that the cloud's behaviour as regards this dimension is unaffected by the slope. However, a cloud which does not spread longitudinally on the slope, but which continues to spread laterally, seems a little outlandish. It would therefore seem pertinent to assume that a solution exists which spreads neither longitudinally nor laterally, but moves down the slope with no change in shape. This is the key to the derivation of the appropriate solution.

3.1.1 Shallow water equations Following the method adopted for the two dimensional case, we take the shallow water theory in the horizontal plane with coordinates $\underline{x}$ in the form

$$\frac{\partial(h-a)}{\partial t} + \underline{\nabla}.(\underline{u}(h-a)) = 0 \tag{3.1}$$

$$\frac{\partial \underline{u}}{\partial t} + (\underline{u}.\underline{\nabla})\underline{u} + g''\underline{\nabla}h = 0 \tag{3.2}$$

with g" as before, and a uniform slope

$$a(\underline{x}) = \Gamma \underline{x}.\underline{\hat{n}} \tag{3.3}$$

where, in keeping with our earlier two–dimensional formalism, we take

$$\underline{\hat{n}} = (-1,0) \tag{3.4}$$

in the (x,y) plane. We shall now show that there is a solution for a cloud of constant uniform velocity, flat top, and fixed shape, exactly as in the two–dimensional case. Figure 3 illustrates this situation.

3.1.2 Solution of the equations In fact it is clear that there is a solution of the equations with

$$\underline{u} = -u\underline{\hat{n}} \tag{3.5}$$

with constant u, and

$$(h - a) = H(\underline{\hat{n}}.(\underline{ut} - \underline{x})) \tag{3.6}$$

with

$$\nabla H = -\Gamma \underline{\hat{n}} \tag{3.7}$$

implying

$$H = \Gamma \underline{\hat{n}}.(\underline{ut} - \underline{x})$$

3.1.3 The boundary condition at the rear The rear of the cloud again has zero depth and, at any given time t, is a straight line across the slope given by

$$\underline{x} = \underline{X}_b(t,y) \tag{3.9}$$

for y in [−Y,+Y], where

$$\underline{X}_b(t,y) = \underline{u}t + (0,y) \tag{3.10}$$

and Y is the overall half-width of the cloud at the trailing edge.

3.1.4 The boundary condition at the front Having thus satisfied the trailing boundary condition, it remains to satisfy the front condition. Let us take the length of the cloud in the direction of the slope to be L(y), as illustrated in the plan view of Figure 4. This is such that L(−y)=L(y); L(Y)=0; and we define L(0)=Λ. The front condition

$$u_f = k_f\sqrt{g'(h-a)_f} \tag{3.11}$$

is now defined for a front velocity component u_f orthogonal to the edge of the cloud. Therefore

$$u_f(y) = \frac{u}{\sqrt{1 + \left(\frac{dL}{dy}\right)^2}} \tag{3.12}$$

at a transverse distance y from the centre line. At this point $(h-a)_f=\Gamma L(y)$, and so, after a little manipulation, the boundary condition gives the equation

$$\frac{dL}{dy} = -\sqrt{\frac{u^2}{k_f^2 g' \Gamma L} - 1} \tag{3.13}$$

from which we deduce

$$\Lambda = \frac{u^2}{k_f^2 g' \Gamma} \tag{3.14}$$

and

$$\frac{d\hat{L}}{d\hat{y}} = -\sqrt{\frac{1 - \hat{L}}{\hat{L}}} \tag{3.15}$$

where

$$\hat{L} = \frac{L}{\Lambda}; \qquad \hat{y} = \frac{y}{\Lambda} \tag{3.16}$$

The solution of this equation may be written parametrically as

$$\hat{L} = \cos^2\omega \tag{3.17}$$

$$\hat{y} = \omega + \cos\omega\sin\omega$$

This shape is illustrated to scale in Figure 5; this completes the three-dimensional generalisation of the simple free-fall cloud presented for two-dimensions in Section 2.

3.1.5 Properties of the solution As we have already noted, the velocity u is related to the overall length Λ of the cloud by

$$u = k_f\sqrt{g'\Gamma\Lambda}$$

As before, it is appropriate to relate this to the volume V of the cloud. This is given by

$$V = \int_{-\frac{\pi}{2}\Lambda}^{+\frac{\pi}{2}\Lambda} dy \int_{0}^{L(y)} dx \,.[\Gamma x] \quad = \Gamma \Lambda^3 \Omega_6 \tag{3.19}$$

where

$$\Omega_6 = \int_{-\frac{\pi}{2}}^{+\frac{\pi}{2}} d\omega \cos^6 \omega \quad = \frac{5\pi}{16} \tag{3.20}$$

Our final result for a cloud of given volume and density is that the free-fall velocity on a slope Γ is

$$u = \Omega_6^{-1/6} . k_f \Gamma^{1/3} \sqrt{g' V^{1/3}} \tag{3.21}$$

This is slightly different from the two-dimensional result. The final factor is again as expected from dimensional analysis, but the slope dependence is now a cube root in place of the fourth root which pertained earlier. It is also interesting to note the prediction that the cloud is π times as wide across the slope as it is long.

Examining the solution, we can again see how a non-spreading cloud can come about. In the longitudinal direction it is exactly as in the 2-dimensional case. The edge velocity is at all points normal to the cloud boundary, but is exactly accounted for by the overall motion of the cloud. At the outside rear edge where the normal points across the slope, the depth and the spreading velocity reach zero together, allowing a non-spreading solution.

3.2 Air entrainment

Modelling air entrainment in the context of the shallow water model is a fairly complicated exercise. A very practical course, however, which is in keeping with the philosophy of simple integral models, is to assume an air entrainment model into a cloud which continues to move on the slope in the above self-similar way. (We shall discuss the possibility of introducing an ambient wind later.) This is not inconsistent with the sort of behaviour discussed by Britter, Cleaver, and Cooper (1991).

In this case the entrainment is assumed just such that the relationship between down-slope velocity u, volume V, and density (implicit in g') is preserved. This allows a very natural generalisation of integral models on flat ground to the case of a uniform slope.

However, if we set out in that direction, any test which we were to apply to the model would depend both on the entrainment model and on the down-slope free-fall model considered here. It would be far preferable if we could test the ideas presented here, independently of the precise details of any entrainment model. In fact we can do this to some extent as is shown in the next section.

4 COMPARISON WITH DATA

4.1 The experiments of Schatzmann et al (1990)

4.1.1 Introduction As part of their contribution to the CEC Major Technological Hazards project Schatzmann, Marotzke, and Donat (1990) used a boundary layer wind tunnel to model an instantaneous release of a dense gas on an inclined plane in conditions of zero ambient flow. This corresponds as closely as possible to the idealisation in our model, and so it is interesting to compare the predictions model with these results. (Steady-continuous releases were also performed, but consideration of these is outside the scope of the model presented here.)

4.1.2 Experimental Set-up In these experiments instantaneous releases were achieved by filling a 450 cm^3 cylinder with a mixture of sulphur hexafluoride (SF_6) and air to the required density and then abruptly retracting the side walls into the wind tunnel floor. Ground level SF_6 concentrations were then measured at eight points down the slope (three on the centre line, five off axis) using artificially aspirated hot-wire anemometers with a sampling rate or either 10 or 12.5 Hz. The concentration time history from each of the sensors is available without additional filtering or averaging.

Each release was repeated five times using identical initial conditions with zero ambient wind. Three different inclines, ranging from Γ=4% to 11.63% (see Figure 1), were also used. Note that the largest of these, Γ=0.1163, is still a shallow slope in the terms discussed earlier.

4.2 Comparison of the model with the data

4.2.1 Model considerations It is desirable to compare the predictions of the model, independently of any particular entrainment model. As it stands in Section 3 the model relates cloud velocity with slope, density and volume without recourse to any free parameters (apart from k_f which is already effectively determined from the cloud spreading law on flat ground). It is therefore our objective to extract these quantities from the data in order to test the predicted relation:

$$u = \Omega_6^{-1/6} . k_f \Gamma^{1/3} \sqrt{g' V^{1/3}} \tag{4.1}$$

obtained above.

4.2.2 Data Reduction In order to do this, we need to know the cloud volume and the relative density excess as a function of time and space. In order to avoid complications which might arise from cross-slope density variations, we have chosen in this study to use only the data from the

three sensors which there placed on the centre line.

For all fifteen instantaneous releases onto inclined planes pure SF_6 was used as the working fluid. Assuming only that this is an isothermal flow of an approximately ideal gas, we know that the flow is buoyancy conserving. That is to say that the cloud-averaged mean density excess

$$\Delta' = \frac{(\bar{\rho} - \rho_a)}{\rho_a} \tag{4.2}$$

is directly proportional to the concentration (contaminant mass per unit volume), and is therefore related to the volume V by

$$\Delta'_0 V_0 = \Delta' V \tag{4.3}$$

where subscript 0 indicates the initial values.

For the moment let us make the bold assumption that we can use the measured concentrations as representative of the mean values, and return to argue about this later. In this case the concentration measurements give immediate estimates of density and volume via these relationships. From these we calculate our model prediction for the cloud velocity u, and test to see whether it agrees with the observed rate of travel.

Schatzmann *et al* present volumetric concentration C as fraction of the initial concentration (C_0) in the cylinder before the release took place. From this we estimate the volume as

$$\frac{V}{V_0} = \left(\frac{C}{C_0}\right)^{-1} \tag{4.4}$$

and find the required combination of variables

$$g' V^{1/3} = g'_0 V_0 V^{-2/3} \tag{4.5}$$

wherein $g'_0 V_0$ can be calculated from the initial conditions. The resultant estimates of the velocity u are given in the tables below, taking the concentration (C) from the mean of the maximum concentrations measured by each sensor during the five repeats, and taking k_f=1.07, a mean spreading Froude number which has been seen (Brighton, Prince and Webber 1985) to optimise fits to Thorney Island (ie flat-gound) data.

Sensor Position	C/C_0	u (ms^{-1})
(61.3,0,0)	$5.826\ 10^{-2}$	0.080
(122.61,0,0)	$1.624\ 10^{-2}$	0.052
(183.91,0,0)	$0.962\ 10^{-2}$	0.044

Table 1: 4.0% Slope

Sensor Position	C/C_0	u (ms^{-1})
(61.3,0,0)	$8.282\ 10^{-2}$	0.361
(122.61,0,0)	$3.188\ 10^{-2}$	0.263
(183.91,0,0)	$1.616\ 10^{-2}$	0.209

Table 2: 8.6% Slope

Sensor Position	C/C_0	u (ms^{-1})
(61.3,0,0)	$8.242\ 10^{-2}$	0.399
(122.61,0,0)	$3.540\ 10^{-2}$	0.301
(183.91,0,0)	$1.464\ 10^{-2}$	0.224

Table 3: 11.63% Slope

We cannot measure the cloud advection velocity directly from the experimental data. We can however, obtain the cloud arrival time at the three sensor locations. By plotting arrival time against distance from the source we do get at least some indication of the cloud velocity, even though there are only three data points for each run. In Figures 6a-6c we have plotted arrival times and drawn a smooth curve through the data to guide the eye. Our predicted velocity is shown as a short line with the appropriate gradient (u) at each data point. If our model were exactly correct, and the extraction of the cloud volume and density accurate, then these lines would be tangents to the curve. Given the uncertainties in the data extraction procedure, we regard the results as sufficiently good to support the shallow water model approach.

It is worth noting that the wedge-shaped flow of our model will take some time to set itself up, and we should therefore expect the model to be better in the far field. The near field data must reflect the initial slumping which is not considered in the model we have presented. It is also interesting that the model seems best when applied to the shallowest slope.

5 DISCUSSION AND CONCLUSIONS

5.1 Significance of the results

Our interpretation of the data is of necessity very crude. The assumption that the measurements reflect the average concentration (or more particularly the concentration which corresponds to the best choice of density in the shallow-water model) looks at first sight to be somewhat cavalier, and to take rather too literally the old box model idea that concentration and density variations are well represented by profiles which are uniform within the cloud and zero outside it.

However, let us now suppose that the profiles are merely self-similar to some reasonable approximation. This is still an assumption of course, but a much weaker one. Self-similarity means that the cloud-average concentration and density are simply constant multiples of the ground-level centre-line value. In particular the combination $\Delta'V$, (where Δ' is now based on the

ground–level centre–line density) would still be constant in the self–similar régime. There is still some uncertainty in evaluating this from the initial (non–self–similar state) but this is reduced by the square root in evaluating the velocity.

All in all then, we regard the comparison shown in Figures 6a–6c as successful to the degree of accuracy which we can expect of the model. In particular the predicted $\Gamma^{1/3}$ dependence is not unrealistic. It is, however, difficult to test the precise form of this slow dependence on a limited data set. Further data on even shallower slopes might be more revealing in this respect.

It is also worth noting that slopes of practical interest may only be up to 1 in 10 or so (Γ=0.1) which are therefore treatable within this framework.

A general insensitivity to the slope is noted by Britter Cleaver and Cooper (1991). They however quote a dependence of the cloud velocity on the slope of $\sin\theta/\theta$ compared to our result of $(\tan\theta)^{1/3}$. Our methods are inappropriate to large slopes, but clearly their expression cannot be valid close to θ=0, and so a direct comparison is difficult. It is made more difficult by the fact that our result is for a cloud of fixed volume and density, whereas Britter et al discuss the velocity of entraining clouds. There is scope for further work here.

5.2 Further comments

There are two possible ways of seeking further confirmation of the model, which we can contemplate here.

5.2.1 Development of integral models One way is to combine the ideas above with a simple computerised model. Entrainment can be introduced in the usual way, although there is clearly some freedom about how exactly to do this. The simplest way of allowing for advection with the wind is to add the slope–generated velocity discussed here to the wind–advection velocity (vectorially). The predictions of such a model could be compared with a wider data–set. Let us emphasise, however, that this approach would be validating a whole combination of different aspects of the model, including entrainment as well as bulk motion, and therefore, whilst having its own benefits, loses some of the advantages of the simple test presented here. A combination of the two approaches is therefore desirable. We are currently pursuing this avenue.

5.2.2 Further qualitative predictions of the model The model presented here has two qualitative aspects which distinguish it from the results of other approaches. In principle these can be tested if appropriate data are obtained.

Firstly, the approach presented here gives rise to a picture of slumping followed by translation for a cloud released from a highish aspect ratio in calm conditions. (By "highish" we mean the régime discussed earlier where the cloud is tall relative to the drop in the slope, but still shallow.) This separation of slumping and translation contrasts with the slumping accompanied by downhill motion found in the models of Deaves and Hall (1990) and Nikmo and Kukkonen (1991). In our approach this is a consequence of the boundary conditions: while the uphill edge depth and the downhill edge depth are the same, the uphill boundary will spread in the same way as the downhill one. The material will rearrange itself within the boundaries so that the centre of mass moves downhill, but only when the depth of the cloud is comparable with the drop in the slope over its length will the overall downhill translation become apparent. Ultimately the gravity spreading is predicted to stop, and any cloud growth will be due purely to the relatively slow process of entrainment. This is illustrated in a two–dimensional numerical solution of the shallow

water model shown in Figures 7a–7f. In this illustration the cloud is started off as close as possible to the parabolic–topped, flat–ground similarity solution variously described by Fannelop and Jacobsen (1984), Wheatley and Webber (1984), Grundy and Rottman (1985) and Webber and Brighton (1986). This shows the onset of a significant deviation from the self–similar behaviour introduced by the slope, and the transition to the "wedge" behaviour described here.

Secondly, the cloud width predicted by the model (in two horizontal dimensions) is π times its overall length. Whilst exact confirmation of this is unlikely given the oversimplicity of some of our assumptions, any experimental visualisation of this flow which showed a cloud to be wide compared to its length would be an interesting support for this approach – we know *a priori* of no other reason why such a result should appear.

Acknowledgements: Financial support for the work presented here has come from the "STEP" programme of the Commission of the European Communities, from the UK Health and Safety Executive, and the Corporate Research programme of AEA Technology, all of which is gratefully acknowledged.

REFERENCES

P W M Brighton, A J Prince, and D M Webber (1985) "Determination of Cloud Area and Patyh from Visual and Concentration Records", J Hazardous Materials 11 pp 155–178

R E Britter, RP Cleaver, & M G Cooper (1991) "Development of a simple model for the dispersion of denser–than–air vapour clouds over real terrain" British Gas Report MRS E 622.

P J H Builtjes (1992) "Research on continuous and instantaneous heavy gas clouds", TNO Report 92–135

D M Deaves & R C Hall, (1990) "The effects of sloping terrain on dense gas dispersion", J Loss Prevention in the Process Industries 3 pp142–145

T K Fannelop & O Jacobsen, (1984) "Gravitational Spreading of Heavy Gas Clouds Instantaneously Released", J. Applied Mathematics and Physics (ZAMP) 35 pp 559–584

R E Grundy & J W Rottman (1985) "The Approach to Self–Similarity of Solutions of the Shallow–Water Equations representing Gravity Current Releases", J. Fluid Mech. 156 pp39–53

S J Jones, D Martin, D M Webber, and T Wren (1991) "The effects of natural and man–made obstacles on heavy gas dispersion – Part II: Dense gas dispersion over complex terrain" SRD Report SRD/CEC/22938/02

J Nikmo & J Kukkonen (1991) "Modelling Heavy Gas Cloud Advection in Complex Terrain" Finnish Meteorological Institute preprint. (See also "A Model for the Advection of a Heavy Gas Cloud on a Slope" in the proceedings of the International Conference and Workshop on Modeleing and Mitigating the Consequences of Accidental Releases of Hazardous Materials", AIChE 1991 – ISBN 0–8169–0492–8, p655, and also J Hazardous Materials *in press*.)

M Schatzmann K Marotzke, & J Donat (1990) "Research on Continuous and Instantaneous Heavy Gas Clouds – Contribution of sub-project EV4T-00210D to the final report of the joint CEC project". University of Hamburg, Meteorological Institute Report 1990.

D M Webber & P W M Brighton, (1986). "Inviscid Similarity Solutions for Slumping for a Cylindrical Tank", Journal of Fluids Engineering, Vol. 108 p238.

C J Wheatley & D M Webber, (1984). "Aspects of the Dispersion of Denser-than-air Vapours Relevant to Gas Cloud Explosions", Commission of the European Communities Report EUR 9592 En.

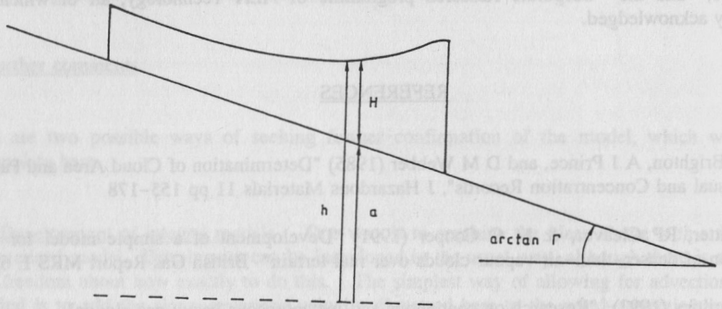

Figure 1 A gas cloud on a slope; definition of geometric variables.

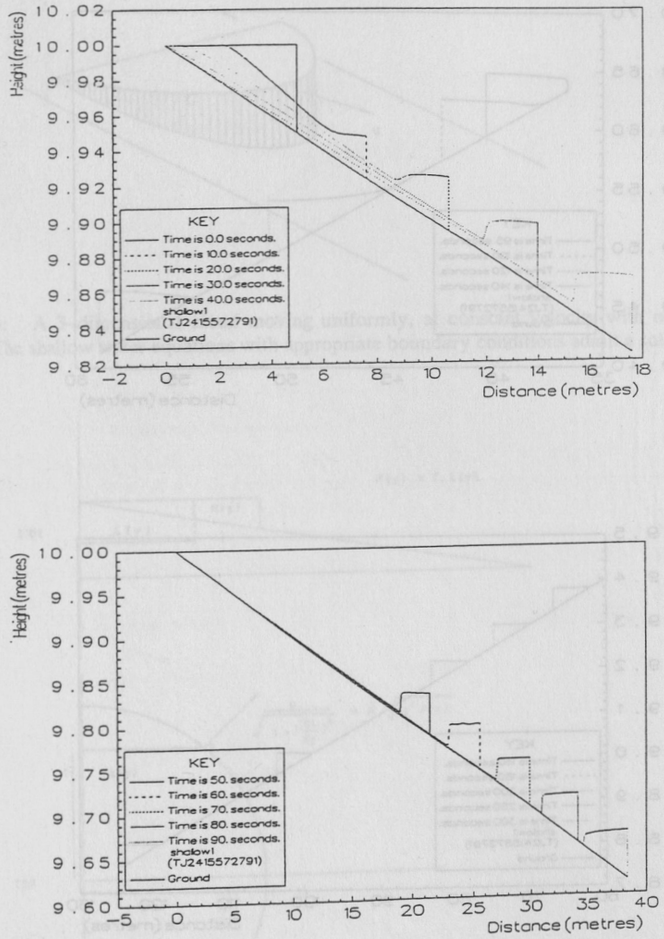

Figure 2a,b: Motion, in 2 dimensions, of a "wedge" released from rest, showing the development of "head" and "tail" regions separated by a hydraulic jump.

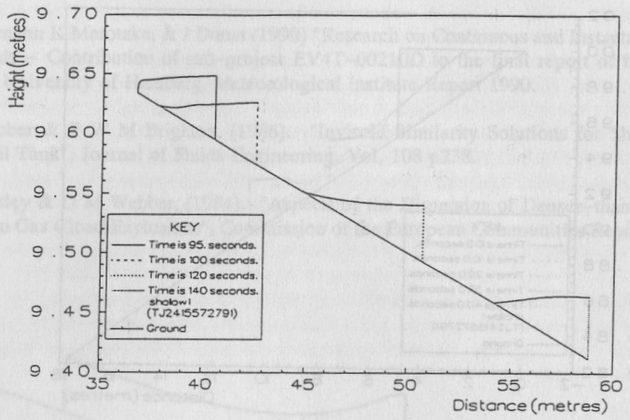

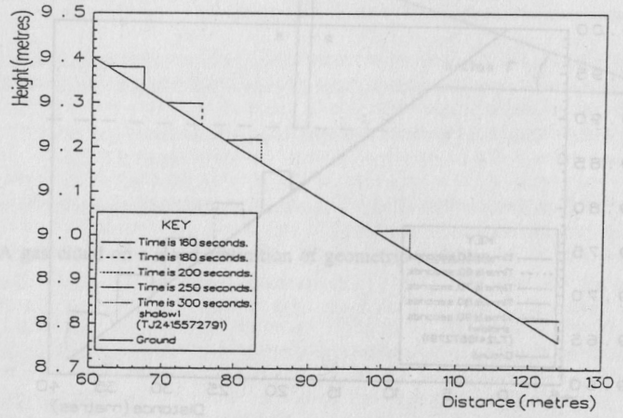

Figure 2c,d: Continued motion, in 2 dimensions, of a "wedge" released from rest, showing the collapse of the hydraulic jump and the formation of a wedge moving uniformly.

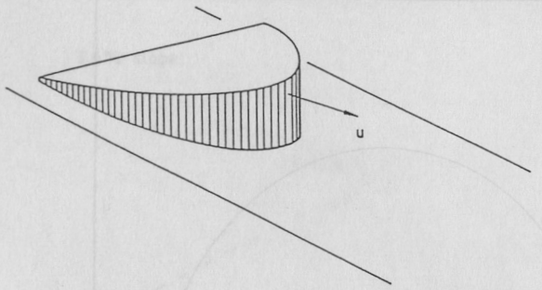

Figure 3: A 3-dimensional cloud moving uniformly, at constant velocity with no change in shape. The shallow water equations with appropriate boundary conditions admit a solution of this form.

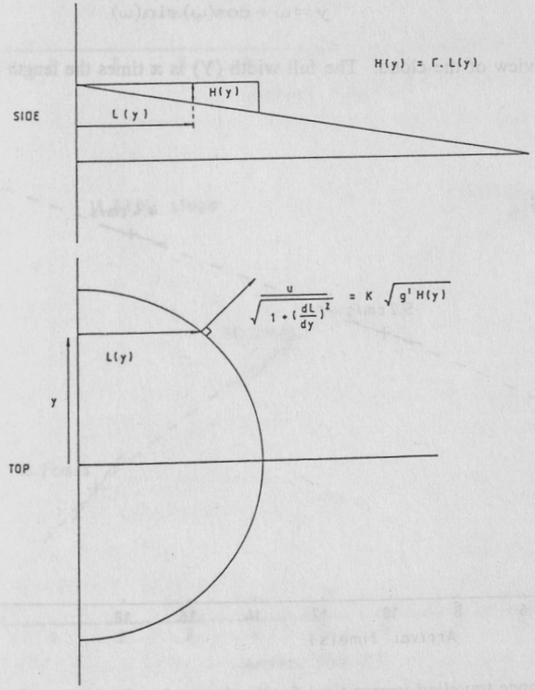

Figure 4: Determination of the shape of the cloud from the boundary conditions.

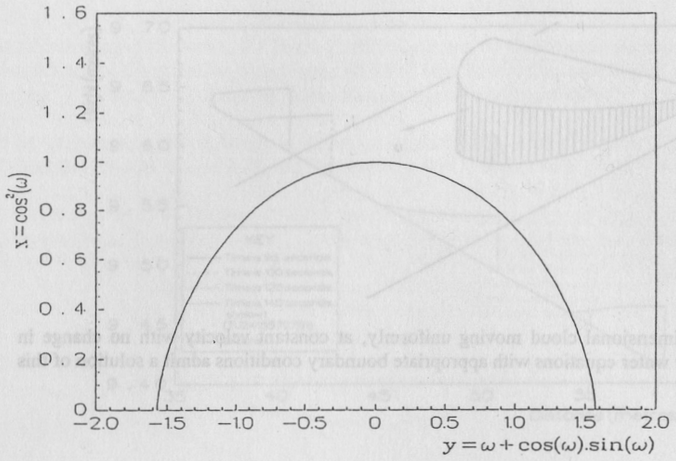

Figure 5: The scaled plan view of the cloud. The full width (Y) is π times the length (X).

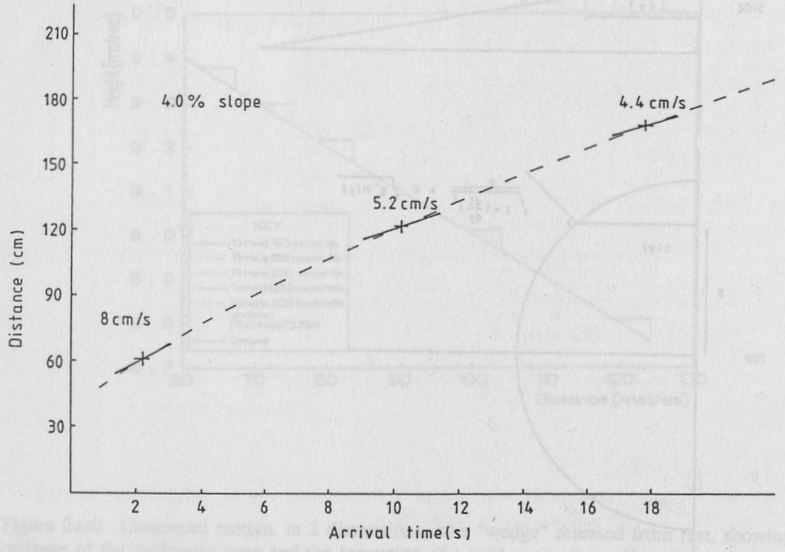

Figure 6a: Centre-line distance travelled versus time for the front of a cloud released at rest on a uniform slope of 0.04. Data are marked (+) and interpolated with a dotted line to guide the eye. The short solid lines indicate the predicted velocity, which if exactly correct, should be tangent to the curve.

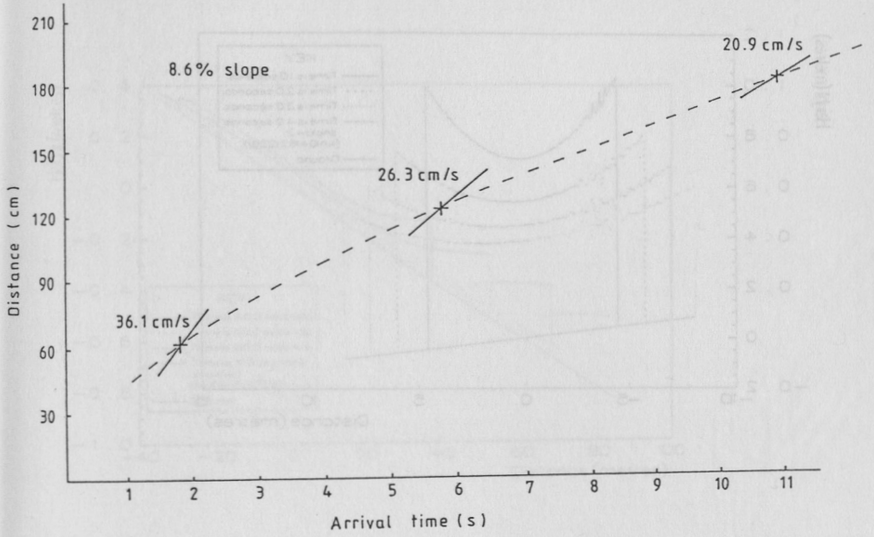

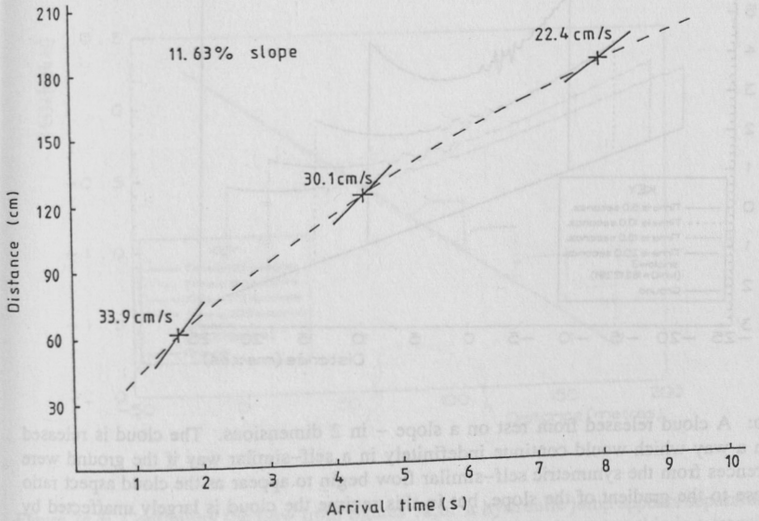

Figures 6b,c: As for figure 6a but with uniform slopes of 0.086 and 0.1163.

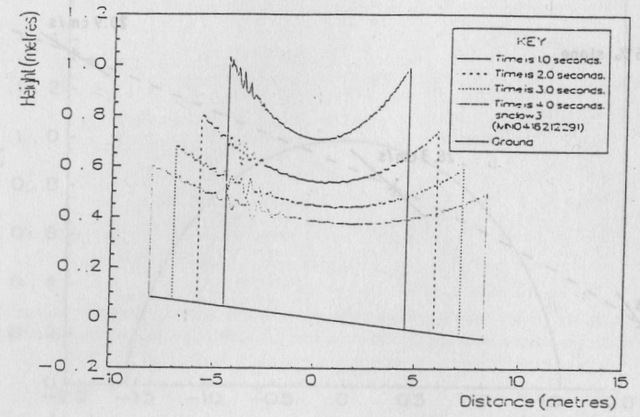

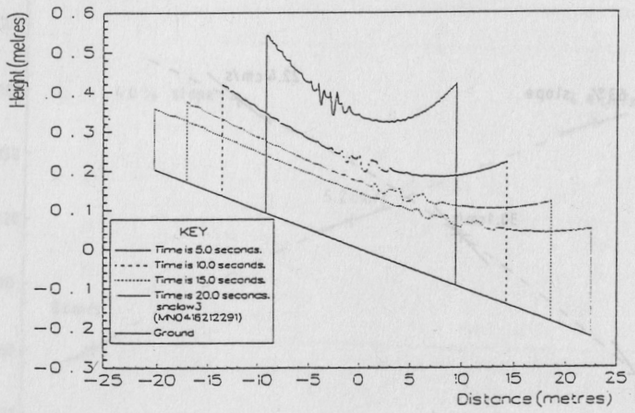

Figures 7a,b: A cloud released from rest on a slope – in 2 dimensions. The cloud is released spreading in a way which would continue indefinitely in a self–similar way if the ground were flat. Differences from the symmetric self–similar flow begin to appear as the cloud aspect ratio becomes close to the gradient of the slope, but in this regime the cloud is largely unaffected by the slope.

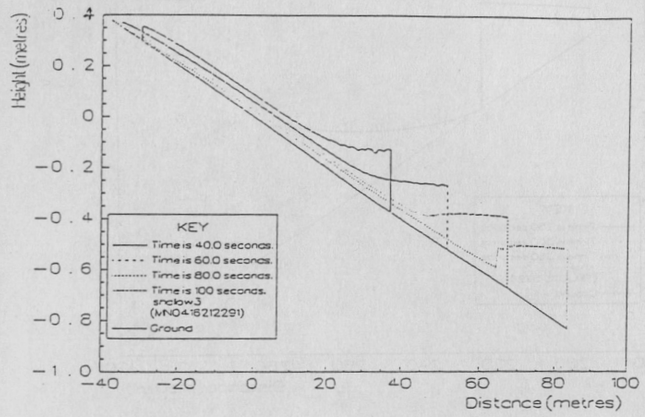

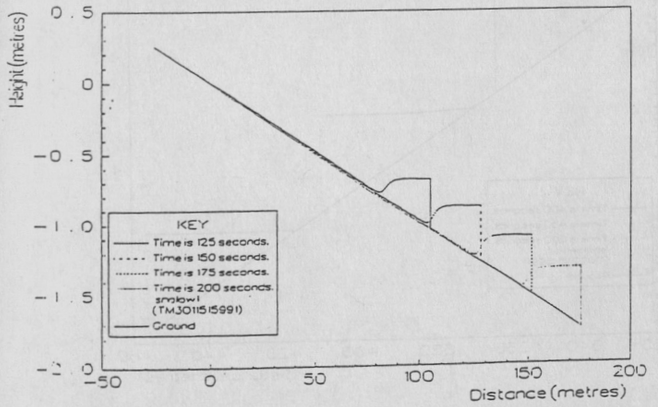

Figure 7c,d: Continuing the flow from figures 7a,b: a hydraulic jump appears separating a "head" and a "tail" region. The slope is having a noticeable effect here, but this is a transition to the final regime.

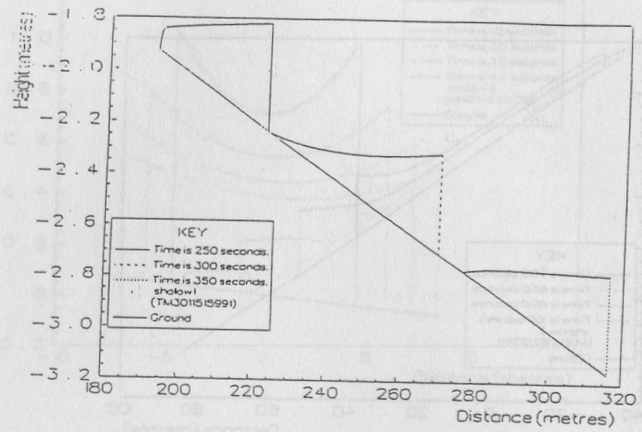

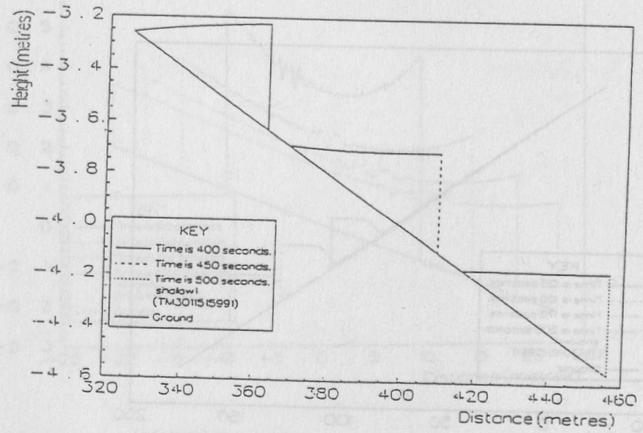

Figures 7e,f: Continuing the flow from Figures 7a–d: in the final regime the hydraulic jump collapses and the cloud reaches the wedge shape which is moving down the hill but no longer spreading.

COMPUTER SIMULATIONS OF WIND AND VENTILATION AID PLATFORM DESIGN AND SAFETY

A. Ronold
DNV Technica, P.O. Box 300, 1322 Høvik, Norway

Computer simulations of wind and ventilation provide a cost efficient tool in the fields of area classification, smoke and gas dispersion and wind-related platform design aspects such as positioning of turbine exhaust and air intakes.

Adequate natural ventilation in petroleum process plants is of crucial importance when classification of hazardous areas is considered. The term "adequate" is most often referring to either the number of air changes in a given area or to the frequency of occurrence of wind speeds less than a given value, typically 0.5 m/s or 2 m/s. In an attempt to specify these parameters accurately, and to aid in the assessment of area classification as well as platform design, computational fluid dynamics (CFD) can be used to simulate the wind flow field and gas or smoke dispersion around and within process plants.

For a given installation, wind simulations are typically carried out for three different wind speeds and eight wind directions. Combined with information from the wind rose for the actual site, these simulations yield the frequency of occurrence of number of air changes on all areas of the installation considered, as well as air velocity distributions. Examples are presented from offshore installations in the North Sea.

Given the wind flow field and air velocity distributions for a certain installation, gas or smoke dispersion simulations can be performed, for example to consider the likelihood of having ignitable gas-air concentrations into non-hazardous areas of the plant in the case of a major gas release. Examples on calculated gas concentration profiles for certain release scenarios are presented.

Keywords: Ventilation, Area Classification, Gas Dispersion, Wind

INTRODUCTION

Wind and ventilation play an important role in many aspects of offshore technology and a thorough understanding of the air flow behaviour is essential in decision making in platform design. This knowledge can be obtained through experiments, but prototype measurements are often impossible for cost and safety reasons, and model experiments such as wind tunnel tests are also expensive and time consuming - and may suffer from scaling problems. Alternatively, numerical simulations may be used to determine the ventilation characteristics of a plant, and at DNV the in-house computer programme COFAN has become increasingly important within the areas of process technology and consequence analyses, and has proven to be an efficient tool for solving problems comprising complex flow phenomena.

COFAN - complex flow analysis - simulates fluid flow, heat and mass transfer in two- and three-dimensional geometries by solving the 'finite volume' versions of the differential equations governing the flow (Navier-Stokes) and using the k-ϵ model of turbulence, as described by Rastogi (1). The 'finite volumes' in question are arrays of contiguos 'cells', each of which possesses a typical value of the pressure, temperature, velocity components, etc. of the fluid. One of the advantages of COFAN is the adaptability to complex geometries. COFAN utilises a technique developed by Karki (2) that makes it possible to generate a body-fitted curvilinear grid, in which